Estimation of Algal Bloom Biomass Using UAV-Based Remote Sensing with NDVI and GRVI

Chanudom Salarux and Siwa Kaewplang*

Faculty of Engineering, Mahasarakham University, Khamriang Sub-district, Kantarawichai District, Maha Sarakham, 44150, Thailand

siwakaewplang@gmail.com*

Abstract. *In this paper, the ability to estimate the biomass of algal bloom by using UAV remote sensing with NDVI and GRVI were compared. Mathematical models such as linear, polynomial and power functions were used to determine the correlation between 2 vegetation indices (NDVI and GRVI) and biomass of algal bloom from field survey. Eighty biomass data from field survey was divided half for calibration and half for evaluation data sets. From mathematical models, the power function provided maximum R^2 both NDVI and GRVI, NDVI give R^2 = 0.72 (RMSE = 38.5) and GRVI give R^2 = 0.64 (RMSE = 42.5) for evaluation datasets, respectively. The results showed that NDVI from UAV remote sensing performed better estimation for biomass of algal bloom than GRVI.*

Received by	2 December 2019
Revised by	28 December 2019
Accepted by	2 January 2020

Keywords: Algal Bloom, Biomass, UAV, NDVI, GRVI

1. Introduction

An algal bloom is natural phenomena that has been happened from the rise of water temperature and pollution in the water environment. [1-4] Harmful algal blooms (HABs) in rivers and lakes, which are resulted from the nutrients such as phosphorus (P) and nitrogen (N), the rise in water temperature, slow river flow, and inland waters. [5-8] HABs may cause the ecosystem to be destroyed, and generation of toxins such as cyanotoxins and microcystins in water [9], which can damage the health of humans and livestock.

The conventional way to obtain the biomass of algal bloom is to use water sampling methods that require manual operation, and recording the result from laboratory. These methods would require large area, long-term measurements challenging and time-consuming. [10]

UAV remote sensing offers an option for collecting data on spatial and spectral resolution, and remote sensing, which has been accepted as the best technique for monitoring algal blooms over large areas.[11-12] Nam-Gu , Lyu, Xu and Bollard-Breen [13-16] refer to that UAVs cost is reasonable in that, they can be more powerful than satellite imagery in both time and money and can reduce in situ water quality sampling costs [17] UAV remote sensing was conducted with RGB camera. [18-20] or RGB + infrared (IR) cameras (multispectral cameras) [13,16,19,21] and hyperspectral sensors. [11-12, 22] Deon Van der Merwe and Kevin [23] using UAV imagery estimated harmful algal bloom biomass by generating a blue normalized difference vegetation index (NDVI). The results show correlations between NDVI and BPCV follow a logarithmic model, with R^2 values from 0.77 to 0.87.

The Normalized Difference Vegetation Index (NDVI), which is a normalized ratio of red and near-infrared reflectance [24], has been used in many phenological studies, including the detection of algal bloom [25-28]. The Green-Red Vegetation Index (GRVI) which is a normalized ratio of red and green reflectance [29-30], has been used to detected plant phenology [31-33]

However, it is surprising that many studies on the application of UAV remote sensing for estimate algal bloom biomass by GRVI have not yet been carried out. Consequently, this study is a pioneering effort to investigate whether UAV-based remote sensing and GRVI can be used to estimate the biomass of algal bloom. The purpose of this study was to assess the use of NDVI and GRVI from UAV remote sensing and compare the performance of different mathematical models such as linear, polynomial and power functions to estimate biomass of algal bloom.

2. Materials and Methods

2.1 Study Area

The study site for this research is located within Mahasarakham University, Mahasarakham Province, Thailand (16°14'51.6"N 103°14'48.4"E), see Fig.1, at an average elevation of 157 m MSL. The study area has a warm temperate semi-humid continental monsoon climate. The average annual temperature is 32.8 °C and the average annual rainfall is 1,202 mm/year.

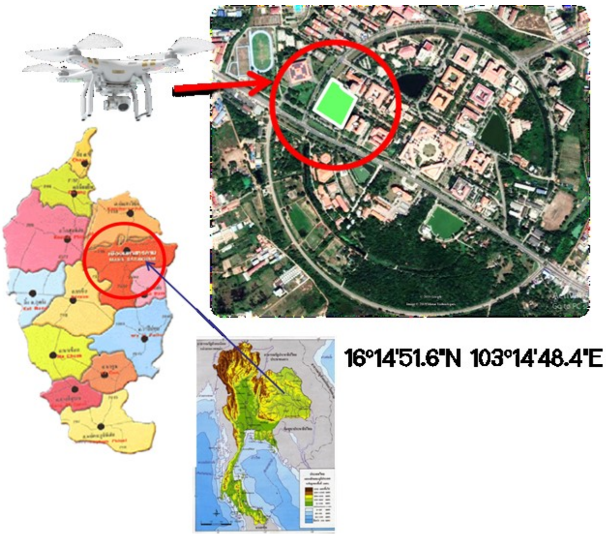

Fig. 1: The location of this study in Mahasarakham University, Mahasarakham Province, Thailand

2.2 Field Data Collection

To identify the appearance of the algae bloom in the reservoir area to examine the results of image detection by NDVI and GRVI from UAV remote sensing, the researcher conducted field investigation 80 plots were used as water sampling on reservoir area to investigate for the biomass of the algal bloom in Environmental Laboratory on November 20th, 2018.

Six ground control points (GCPs) distributed around the field were used to obtain accurate geographical references and were located with not less 4 cm. accuracy by using a GNSS.

2.3 Unmanned aerial vehicle and camera setup

The digital imagery was collected with the DJI Phantom 3 professional. Digital imagery was collected by using a 1.2 megapixel camera, which captures three discrete spectral bands: blue (wavelength = 450 nm), green (wavelength = 550 nm), and red (660 nm) (Fig. 2) and The Survey3 cameras, which captures three discrete spectral bands: Red Green NIR (Fig. 3) model sees Near Infrared 850 nm, Red 660 nm, and Green 550 nm light. The radiometric calibration images of DJI camera were captured on the ground before and after each flight by using a calibrated reflectance panel. Flight paths over the trial area were designed by PIX4D Capture. The forward overlap was 80% and the lateral overlap was 60%. The flight speed was fixed at 6 m/s. ISO and shutter speed were fixed at 160 and 1/2000, respectively. The flight altitude above ground level (AGL) on November 10th, 2018 was 50 m. The ground sampling distances for digital imagery were approximately 2.19 cm.

2.4 Image processing and data extraction

Web ODM was used to generate orthomosaics and six ground control points were used to geometric correction. Radiometric calibration was done by using radiometric calibration images with known reflectance values. The radiometric corrections were used to improve the radiometric quality of the data and correct the reflectance of the image. The images from Survey3 cameras (RGN) are commonly calibrated into an index image and then a colored is applied to show the contrast between healthy and poor health vegetation.

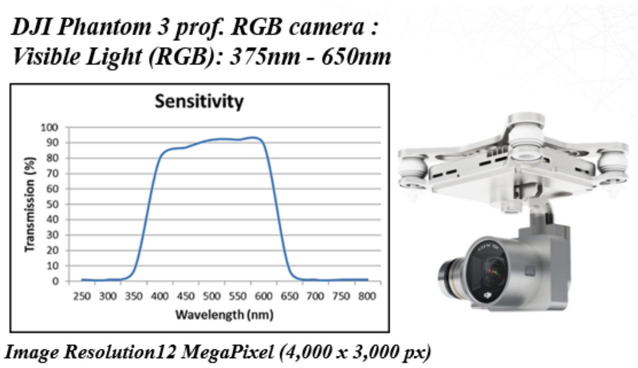

Fig. 2: DJI Phantom 3 professional camera (RGB)

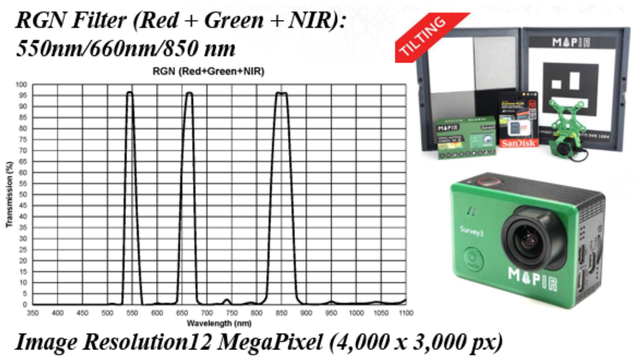

Fig. 3: The Survey3 cameras (RGN)

3. Modeling and resampling

To achieve the suitable to a mathematical model by a comparative analysis of NDVI and GRVI values for estimating biomass of algae bloom, we establish three mathematical models. Linear regression, polynomial and power functions models are stringent in requiring predictor variables, so data pre-processing techniques should be performed on the training set before modeling.

The coefficient of determination (R^2), and RMSE were used as assessment metrics to measure the performance of the mathematical model and to determine how good the model predicts new data. Equations (1)-(2) are used to calculate R^2, and RMSE.

$$R^2 = 1 - \frac{\sum_{i=1}^{N} (y_i - \hat{y}_i)^2}{\sum_{i=1}^{N} (y_i - \bar{y}_i)^2} \quad (1)$$

$$\mathrm{RMSE} = \sqrt{\frac{1}{N}\sum_{i=1}^{N} (y_i - \hat{y}_i)^2} \quad (2)$$

; where N is the total sample size; y_i is the ith measured biomass of the sample; $y\hat{}_i$ is the ith predicted value, and $y\bar{}_i$ is the ith mean measured value.

4. Results

The average field biomass value measured in the field was 425 mg/l (N = 80, SD = 32.5). The R^2 values of the Linear regression, polynomial and power functions models are reported in Table 1 and Table 2. The power function gives the maximum R^2 both NDVI and GRVI, NDVI gives $R^2 = 0.72$ (RMSE = 38.5) and GRVI gives $R^2 = 0.64$ (RMSE = 42.5) for evaluation datasets respectively.

Model	Training Set		Test Set	
	R^2	RMSE	R^2	RMSE
Linear regression	0.62	46.3	0.65	42.5
Polynomial	0.65	44.5	0.68	40.5
power functions	0.68	40.2	0.72	38.5

Table 1 The R^2 values and the RMSE values of NDVI models indicating P<0.01

Model	Training Set		Test Set	
	R^2	RMSE	R^2	RMSE
Linear regression	0.52	48.6	0.55	46.2
polynomial	0.55	45.5	0.58	44.5
power functions	0.60	45.2	0.64	42.5

Table 2 The R^2 values and the RMSE values of GRVI models indicating P<0.01

The plots of the biomass of algae bloom estimated by power functions model are showed in Fig. 4 (objects outside the study areas are masked out) and Scatter plots of observed the biomass of algae bloom versus predicted the biomass of algae bloom for validation data are shown in Fig. 5 and Fig. 6. This study used A one-way ANOVA test and was also used for testing the similarity between the regression models when three different models were used. It turned out that the three models are statistically not different. (i.e., p-value<0.01, N = 80)

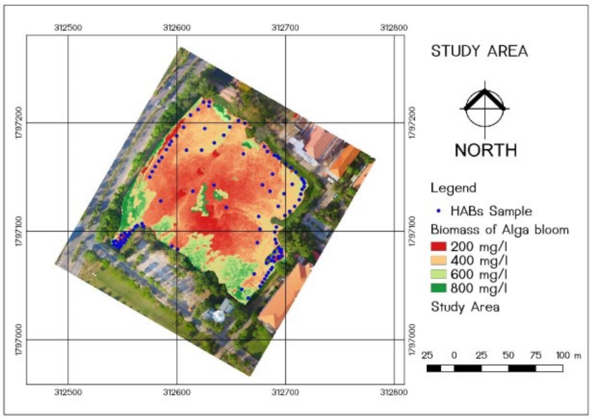

Fig. 4: The biomass of algae blooms map estimated using random forest models.

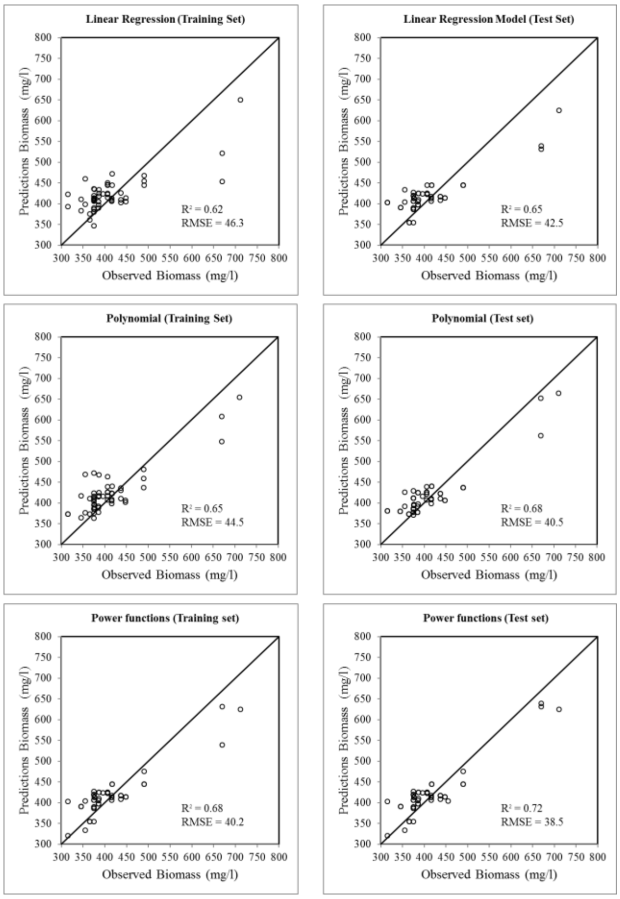

Fig. 5: The scattering plots with the RMSE values of Biomass - NDVI models

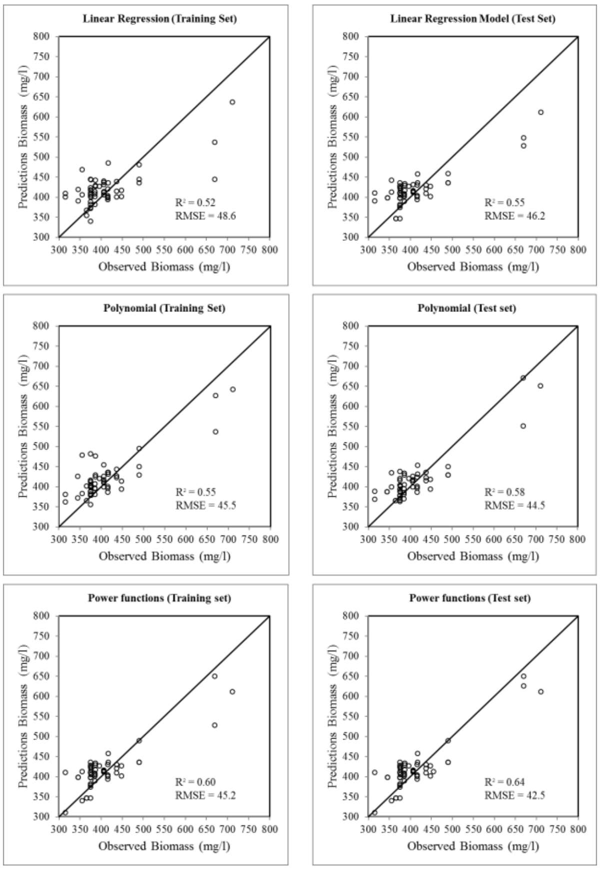

Fig. 6 : The scattering plots with the RMSE values of Biomass-GRVI models

5. Discussion and Conclusion

The result of this study from the recorded UAV-derived aerial imagery from an RGB and RGN camera data can be used for estimating biomass of algal bloom from NDVI and GRVI. (please see Table 1-2 and Fig. 5-6) Strong statistical correlations of algae bloom biomass models from power functions models agree with early studies of algae bloom biomass [11-15,17-19]. The aim of this study to report simple linear and non-linear correlations between NDVI and GRVI derived from the RGB camera and RGN from survey 3 camera and biomass of algal bloom values collected from the field. This report is not to provide a thorough analysis. The results could be improved by machine learning algorithm [30,33-35]. It is concluded that the NDVI model is the most suitable model for inverting biomass of alga bloom in the study area. However, the NDVI inversion model must avoid a saturation phenomenon when NDVI is close to 1. Consequently, we expect the methodology in this study can useful guidelines for estimating and biomass of algal bloom.

Acknowledgements

This study was supported by, Faculty of Engineering, Mahasarakham University, Thailand.

References

[1] Senhorst, H. A. J., & Zwolsman, J. J. (2005). Climate change and effects on water quality: a first impression. Water Science and Technology, 51(5), 53-59.

[2] Thackeray, S. J., Jones, I. D., & Maberly, S. C. (2008). Long-term change in the phenology of spring phytoplankton: species-specific responses to nutrient enrichment and climatic change. Journal of Ecology, 96(3), 523-535.

[3] Kim, H. (2010). An overview on the occurrences of harmful algal blooms (HABs) and mitigation strategies in Korean coastal waters. Coastal environmental and ecosystem issues of the east china sea, 121-131.

[4] Van der Merwe, D., & Price, K. (2015). Harmful algal bloom characterization at ultra-high spatial and temporal resolution using small unmanned aircraft systems. Toxins, 7(4), 1065-1078.

[5] Matthews, M. W. (2009). Remote sensing of water quality parameters in Zeekoevlei, a hypertrophic, cyanobacteria-dominated lake, Cape Town, South Africa (Doctoral dissertation, University of Cape Town).

[6] Hallegraeff, G. M. (2003). Harmful algal blooms: a global overview. Manual on harmful marine microalgae, 33, 1-22.

[7] Kirkpatrick, B., Fleming, L. E., Squicciarini, D., Backer, L. C., Clark, R., Abraham, W., ... & Zaias, J. (2004). Literature review of Florida red tide: implications for human health effects. Harmful algae, 3(2), 99-115.

[8] Jung, S., Cho, H., Kim, D., Kim, K., Han, J. I., & Myung, H. (2017). Development of algal bloom removal system using unmanned aerial vehicle and surface vehicle. IEEE Access, 5, 22166-22176.

[9] Zhang, K., Lin, T. F., Zhang, T., Li, C., & Gao, N. (2013). Characterization of typical taste and odor compounds formed by Microcystis aeruginosa. Journal of Environmental Sciences, 25(8), 1539-1548..

[10] Smayda, T. J. (1997). What is a bloom? A commentary. Limnology and Oceanography, 42(5part2), 1132-1136.

[11] Honkavaara, E., Hakala, T., Kirjasniemi, J., Lindfors, A., Mäkynen, J., Nurminen, K., ... & Markelin, L. (2013). New light-weight stereoscopic spectrometric airborne imaging technology for high-resolution environmental remote sensing case studies in water quality mapping. Int. Arch. Photogram. Remote Sens. Spat. Inf. Sci, 1, W1.

[12] Pölönen, I., Puupponen, H. H., Honkavaara, E., Lindfors, A., Saari, H., Markelin, L., ... & Nurminen, K. (2014, October). UAV-based hyperspectral monitoring of small freshwater area. In Remote Sensing for Agriculture, Ecosystems, and Hydrology XVI (Vol. 9239, p. 923912). International Society for Optics and Photonics.

[13] Nam-Gu, B., CO, L., Jungangdae-ro, D. G., & Gwanganhaebyeon-ro, S. G. (2016). Application of Unmanned Aerial Vehicle Imagery for Algal Bloom Monitoring in River Basin. International Journal of Control and Automation, 9(12), 203-220.

[14] Lyu, P., Malang, Y., Liu, H. H., Lai, J., Liu, J., Jiang, B., ... & Wang, Y. (2017). Autonomous cyanobacterial harmful algal blooms monitoring using multirotor UAS. International journal of remote sensing, 38(8-10), 2818-2843.

[15] Xu, F., Gao, Z., Jiang, X., Shang, W., Ning, J., Song, D., & Ai, J. (2018). A UAV and S2A data-based estimation of the initial biomass of green algae in the South Yellow Sea. Marine pollution bulletin, 128, 408-414.

[16] Bollard-Breen, B., Brooks, J. D., Jones, M. R., Robertson, J., Betschart, S., Kung, O., ... & Pointing, S. B. (2015). Application of an unmanned aerial vehicle in spatial mapping of terrestrial

biology and human disturbance in the McMurdo Dry Valleys, East Antarctica. Polar biology, 38(4), 573-578.

[17] Koparan, C., Koc, A., Privette, C., & Sawyer, C. (2018). In situ water quality measurements using an unmanned aerial vehicle (UAV) system. Water, 10(3), 264.

[18] Su, T. C., & Chou, H. T. (2015). Application of multispectral sensors carried on unmanned aerial vehicle (UAV) to trophic state mapping of small reservoirs: a case study of Tain-Pu reservoir in Kinmen, Taiwan. Remote Sensing, 7(8), 10078-10097.

[19] Jang, S. W., Yoon, H. J., Kwak, S. N., Sohn, B. Y., Kim, S. G., & Kim, D. H. (2016). Algal bloom monitoring using UAVs imagery. Adv. Sci. Technol. Lett, 138, 30-33.

[20] Aguirre-Gómez, R., Salmerón-García, O., Gómez-Rodríguez, G., & Peralta-Higuera, A. (2017). Use of unmanned aerial vehicles and remote sensors in urban lakes studies in Mexico. International journal of remote sensing, 38(8-10), 2771-2779.

[21] Goldberg, S. J., Kirby, J. T., & Licht, S. C. (2016). Applications of Aerial Multi-Spectral Imagery for Algal Bloom Monitoring in Rhode Island. SURFO Technical Report No. 16-01, 28.

[22] Shang, S., Lee, Z., Lin, G., Hu, C., Shi, L., Zhang, Y., ... & Yan, J. (2017). Sensing an intense phytoplankton bloom in the western Taiwan Strait from radiometric measurements on a UAV. Remote Sensing of Environment, 198, 85-94.

[23] Van der Merwe, D., & Price, K. (2015). Harmful algal bloom characterization at ultra-high spatial and temporal resolution using small unmanned aircraft systems. Toxins, 7(4), 1065-1078.

[24] Kiage, L. M., & Walker, N. D. (2009). Using NDVI from MODIS to monitor duckweed bloom in Lake Maracaibo, Venezuela. Water resources management, 23(6), 1125-1135.

[25] Son, Y. B., Min, J. E., & Ryu, J. H. (2012). Detecting massive green algae (Ulva prolifera) blooms in the Yellow Sea and East China Sea using geostationary ocean color imager (GOCI) data. Ocean Science Journal, 47(3), 359-375.

[26] Li, Y., Zhang, L. F., Huang, C. P., Wang, J. N., & Cen, Y. (2016). Monitor of cyanobacteria bloom in Lake Taihu from 2001 to 2013 based on MODIS temporal spectral data. Guang pu xue yu guang pu fen xi= Guang pu, 36(5), 1406-1411.

[27] Hu, C. (2009). A novel ocean color index to detect floating algae in the global oceans. Remote Sensing of Environment, 113(10), 2118-2129.

[28] Tucker, C. J. (1979). Red and photographic infrared linear combinations for monitoring vegetation. Remote sensing of Environment, 8(2), 127-150.

[29] Falkowski, M. J., Gessler, P. E., Morgan, P., Hudak, A. T., & Smith, A. M. (2005). Characterizing and mapping forest fire fuels using ASTER imagery and gradient modeling. Forest Ecology and Management, 217(2-3), 129-146.

[30] Suphan, P., Sa-ngiamvibool, W & Kaewplang, S. (2019). Monitoring of Rice Growth with UAV-derived aerial imagery.

[31] Rau, J. Y., Jhan, J. P., Lo, C. F., & Lin, Y. S. (2011). Landslide mapping using imagery acquired by a fixed-wing UAV. Int. Arch. Photogramm. Remote Sens. Spat. Inf. Sci, 38(1/C22), 195-200.

[32] Nagai, S., Saitoh, T. M., Nasahara, K. N., Inoue, T., & Suzuki, R. (2015, December). Accurate detection of spatio-temporal variability of plant phenology by using satellite-observed daily green-red vegetation index (GRVI) in Japan. In AGU Fall Meeting Abstracts.

[33] Ali, I., Greifeneder, F., Stamenkovic, J., Neumann, M., & Notarnicola, C. (2015). Review of machine learning approaches for biomass and soil moisture retrievals from remote sensing data. Remote Sensing, 7(12), 16398-16421.

[34] Han, L., Yang, G., Dai, H., Xu, B., Yang, H., Feng, H., ... & Yang, X. (2019). Modeling maize above-ground biomass based on machine learning approaches using UAV remote-sensing data. Plant methods, 15(1), 10.

[35] Yang, S., Feng, Q., Liang, T., Liu, B., Zhang, W., & Xie, H. (2018). Modeling grassland above-ground biomass based on artificial neural network and remote sensing in the Three-River Headwaters Region. Remote Sensing of Environment, 204, 448-455.

Biographies

Chanudom Salarux received his bachelor's degree in Civil Engineering from North Eastern University, Thailand. He is a civil engineer in Khok Phra Sub-district Municipality, Kantharawichai District, Maha Sarakham Province, Thailand.

Siwa Kaewplang was born in Thailand. He received his Phd. from Chulalongkorn University in 2014. He is a lecturers of Civil engineering at Mahasarakham University, Thailand. His research interests include Digital Photogrammetry; Climate Change; Environmental modeling; Geographic Information System; Geostatistics; GIS; Global warming; Remote Sensing Hyperspectral remote sensing; Image classification; Image processing ; Information technology ; Precision agriculture; Natural resource management; Tropical forest; Tropical vegetation; Water resource management.